Journal of Macromolecular Science®, Part A: Pure and Applied Chemistry, 43:1635–1649, 2006

ISSN 1060-1325 print/1520-5738 online
DOI: 10.1080/10601320600897056

Phase Transition of Acrylamide-Based Polyampholyte Gels in Water

DENIZ CEYLAN, VOLKAN CAN, AND OGUZ OKAY

Department of Chemistry, Istanbul Technical University, Istanbul, Turkey

The swelling behavior of acrylamide (AAm)–based polyampholyte hydrogels in water and in aqueous salt (NaCl) solutions was investigated. [(Methacrylamido)propyl]trimethyl-ammonium chloride (MAPTAC) and acrylic acid (AAc) were used as the ionic comonomer in the hydrogel preparation. Three sets of hydrogels containing 70 mol% AAm and 30 mol% ionic comonomers of varying mole ratios were prepared. The variations of the hydrogel volume in response to changes in pH, and salt concentration were measured. As pH increases from 1, the hydrogel volume V_{eq} *in water first increases and reaches a maximum value at a certain pH. Then, it decreases again with a further increase in pH and attains a minimum value around the isoelectric point (IEP). After passing the collapsed plateau region, the gel reswells again up to* $pH = 7.1$. *The reswelling of the collapsed gels containing 10 and 4% MAPTAC occurs as a first-order phase transition at* $pH = 5.85$ *and 4.35, respectively, while the hydrogel with 1% MAPTAC reswells continuously beyond its IEP. Depending on pH of the solution, the hydrogels immersed in salt solutions exhibit typical polyelectrolyte or antipolyelectrolye behavior. The experimental swelling data were compared with the predictions of the Flory-Rehner theory of swelling equilibrium including the ideal Donnan equilibria. It was shown that the equilibrium swelling theory qualitatively predicts the experimental behavior of polyampholyte hydrogels.*

Keywords polyampholyte gels, acrylamide, swelling, isoelectric point, phase transition

Introduction

Polyampholyte hydrogels are swollen crosslinked polymer networks containing both positively and negatively charged monomer units (1–4). Such materials are usually prepared by crosslinking copolymerization of two ionic comonomers having oppositely charged functional groups. The net charge in a polyampholyte hydrogel can be adjusted by changing the composition of the comonomer feed solution. If the net charge is large, the hydrogel behaves like a conventional polyelectrolyte in which the osmotic pressure of the counter ions plays a major role. In a balanced polyampholyte hydrogel, that is, if the hydrogel contains equal numbers of positive and negative monomer units, the net electrostatic forces are attractive so that, in water, the network chains have a tendency to collapse into a compact globule. The addition of salt screens these attractive interactions and induces a gel swelling. Therefore, unlike polyelectrolytes, balanced polyampholyte

Received February 2006; Accepted April 2006.
Address correspondence to Oguz Okay, Department of Chemistry, Istanbul Technical University, Maslak, 34469 Istanbul, Turkey. E-mail: okayo@itu.edu.tr

hydrogels have the unique capacity to swell in aqueous solutions of high ionic strengths. This so-called antipolyelectrolyte property has a number of important implications for their technological use. Such materials are also attractive for theoretical studies since they provide a model for studying the long-range interactions found in proteins.

Prausnitz et al. investigated the swelling behavior of polyampholyte hydrogels based on [(Methacrylamido)propyl]trimethylammonium chloride (MAPTAC) and sodium styrene sulfonate (SSS) comonomers (1, 2). They showed that the ideal Donnan theory describes qualitatively the swelling behavior of the hydrogels in water and in NaCl solutions. Nisato et al. reported that the degree of charge imbalance of the gel network determines the properties of polyampholyte hydrogels (3). Takeoka et al. observed first-order phase transitions in MAPTAC/SSS hydrogels immersed in water-organic solvent mixtures (5). English et al. showed that the collapse transitions in polyampholyte hydrogels at low and intermediate salt concentrations could be predicted by the equilibrium theory of swelling including the Donnan equilibria (6). In all the studies mentioned above, the net charge in polyampholyte hydrogels was varied by changing the comonomer feed composition. This procedure, however, alters the formation history of gels, which may lead to different gel morphologies affecting their physical properties (7, 8). An alternative approach is to use a weak electrolyte as one of the ionic comonomers in the hydrogel preparation (4, 9, 10). In this case, the net charge can be adjusted by changing pH of the swelling medium without affecting the gel formation history. Annaka and Tanaka investigated the swelling behavior of hydrogels consisting of MAPTAC and acrylic acid (AAc) units (9). They observed the existence of several gel phases in equilibrium with water. Later, it was shown that the phases mainly appear due to the non-equilibrium between the mobile ions inside the gel with those in the external solution (11).

In the present work, we report results of the equilibrium swelling properties of acrylamide (AAm)–based polyampholyte hydrogels. MAPTAC and AAc were used as the cationic and anionic comonomers, respectively. MAPTAC, a quarternized ammonium salt, strongly dissociates in aqueous solutions, rendering the degree of swelling insensitive to pH. However, AAc is a weakly dissociating electrolyte and the degree of dissociation depends on the pH of the solution. Thus, varying pH of the solution can simply monitor the net charge of the hydrogels. It should be noted that, at high charge densities, the counterion condensation, as well as the limited extensibility of the network chains increase the complexity of the theoretical treatment of hydrogel systems. In order to simplify the theoretical treatment, we decreased the network charge density by including the nonionic acrylamide monomer into the comonomer mixture. Here, we prepared three sets of hydrogels containing 70 mol% AAm and 30 mol% ionic comonomers of varying mole ratios. The variations of the hydrogel volume in response to changes in pH, and salt concentration were measured. The results were interpreted within the framework of the equilibrium theory of swelling of ionic hydrogels including the ideal Donnan equilibria.

Experimental

Materials

Acrylic acid (AAc, Fluka) was distilled under a reduced pressure of 10 mm Hg to remove its inhibitor. Acrylamide (AAm, Merck), [(Methacrylamido)propyl]trimethylammonium chloride (MAPTAC) (50% solution in water, Aldrich), N,N′-methylenebis(acrylamide)

(BAAm, Merck), ammonium persulfate (APS, Merck), and N,N,N′,N′-tetramethylethylenediamine (TEMED, Merck) were used as received. APS and TEMED stock solutions were prepared by dissolving 0.160 g APS and 0.250 mL TEMED separately in 10 mL of water.

Synthesis of Hydrogels

Hydrogels were prepared by free-radical crosslinking copolymerization of AAm, MAPTAC and AAc monomers with a small amount of BAAm in aqueous solution at 5°C. The reaction time was 24 h. APS (7.02 mM) and TEMED (0.25 ml/100 ml reaction solution) were used as the redox initiator system. In our experiments, both the crosslinker ratio (mole ratio of the crosslinker BAAm to the monomers) and the total monomer concentration were fixed at 1/80 and 5 w/v%, respectively. The AAm content of the monomer mixture was also fixed at 70 mol%, while the molar ratio of the ionic comonomers was varied.

To illustrate the synthetic procedure, we give details for the preparation of the hydrogel with 10 mol% MAPTAC and 20 mol% AAc in the comonomer feed composition, designated as 10/20-gel: AAm (0.282 g), MAPTAC solution (0.250 g), AAc (0.0817 g), BAAm (0.0109 g), and TEMED stock solution (1 mL) were dissolved in 9 mL of distilled water. After bubbling nitrogen for 20 min, 1 mL of APS stock solution was added and the solution was poured into several glass tubes of 4 mm internal diameters and about 100 mm long. The glass tubes were sealed, immersed in a thermostated water bath at 5°C and the polymerization was conducted for one day. After the reaction, the hydrogels were cut into specimens of approximately 10 mm in length and immersed in a large excess of distilled water for 1 day to remove the unreacted species. Extraction tests conducted at room temperature showed that the conversion of the monomers to the crosslinked polymer was complete after the copolymerization.

Swelling Measurements

Swelling measurements were carried out at 24 ± 0.5°C in water and in NaCl solutions of varying pH between 1 and 11. To obtain various pH between 1 and 11, dilute HCl or NaOH solutions were added into the distilled water. pH of the solutions was measured using the pH meter inoLab (WTW, Germany) with pH electrodes calibrated using three buffer solutions of varying pH. The hydrogels after preparation in the form of rods of 4 mm in diameter were cut into samples of about 10 mm length. Then, each sample was placed in an excess of water at 24 ± 0.5°C. In order to reach swelling equilibrium, the hydrogels were immersed in water for at least one week replacing the water every other day. The swelling equilibrium was tested by measuring the diameter of the gel samples. To achieve good precision, three measurements were carried out on samples of different length taken from the same gel. The normalized volume of the equilibrium swollen hydrogels V_{eq} (volume of equilibrium swollen gel/volume of the gel just after preparation) was determined by measuring the diameter of the hydrogel samples by a calibrated digital compass (Mitutoyo Digimatic Caliper, Series 500, resolution: 0.01 mm). V_{eq} was calculated as

$$V_{eq} = (D/D_0)^3 \tag{1}$$

where D and D_0 are the diameter of hydrogels after equilibrium swelling in water and after synthesis, respectively. The hydrogels equilibrium swollen in water were then transferred into solutions of various pH and the swelling measurements were conducted as described above. To prevent non-equilibrium states in gels (9), the gel samples were always transferred from neutral (water) to acidic or to basic solutions in steps of less than pH = 0.5.

Mechanical Measurements

Uniaxial compression measurements were performed on gels just after their preparation, as well as on equilibrium swollen gels in water. All the mechanical measurements were conducted in a thermostated room of 24 ± 0.5°C. The stress-strain isotherms were measured by using an apparatus previously described (12). Briefly, a cylindrical gel sample of about 7 mm in length was placed on a digital balance (Sartorius BP221S, readability and reproducibility: 0.1 mg). A load was transmitted vertically to the gel through a rod fitted with a PTFE end-plate. The compressional force acting on the gel was calculated from the reading of the balance. The resulting deformation was measured after 20 sec of relaxation by using a digital comparator (IDC type Digimatic Indicator 543–262, Mitutoyo Co.), which was sensitive to displacements of 10^{-3} mm. The measurements were conducted up to about 15% compression. Reversibility of the isotherms was tested by recording the force and the resulting deformation during both force – increasing and force – decreasing processes. The two processes yielded almost identical stress–strain relations. From the repeated measurements, the standard deviations in the modulus value were less than 3%. The elastic modulus G was determined from the slope of linear dependence:

$$F = G(\lambda - \lambda^{-2}) \tag{2}$$

where F is the force acting per unit cross-sectional area of the undeformed gel specimen, G is the modulus of elasticity, and λ is the deformation ratio (deformed length/initial length). For a homogeneous network of Gaussian chains, the elastic modulus of gels G is related to the network crosslink density ν_e by (13, 14):

$$G = A\nu_e RT(\nu_2^0)^{2/3}(\nu_2)^{1/3} \tag{3}$$

where ν_2^0 and ν_2 are the volume fractions of crosslinked polymer after preparation and at the state of the equilibrium swelling, respectively ($\nu_2 = \nu_2^0/V_{eq}$), R and T are in their usual meaning. The front factor A equals to 1 for an affine network and $1-2/\phi$ for a phantom network, where ϕ is the functionality of the crosslinks (15). Since $\nu_2 = \nu_2^0$ for the hydrogels just after preparation, the modulus G_0 after preparation becomes

$$G_0 = A\nu_e RT\nu_2^0 \tag{4}$$

Results and Discussion

Polyampholyte hydrogels were prepared at a fixed initial monomer concentration and the crosslinker ratio but at various molar ratio of the ionic comonomers. The composition of the hydrogels is shown in Table 1. The hydrogels were designated as X/Y-gels, where X and Y denote the mole percent of MAPTAC and AAc units in the network chains. Three sets of gels designated by 10/20-, 4/26-, and 1/29-gels were prepared and subjected to swelling tests in water, as well as in NaCl solutions of various pH. For a given X/Y-gel immersed in water, the isoelectric point (IEP), that is, the point at which the number of dissociated AAc units equals to the number of MAPTAC units should occur if the dissociation degree α of AAc becomes equal to X/Y. Further, since α of a weak

Table 1

Composition of polyampholyte hydrogels. MAPTAC, AAc, and AAm mol% are the percent compositions of the comonomer mixtures used in the hydrogel preparation. pH_{IEP} is the pH, calculated using Equation (5), at which the gel is in its IEP

Hydrogel code	MAPTAC (mol%)	AAc (mol%)	AAm (mol%)	pH_{IEP}
10/20	10	20	70	4.25
4/26	4	26	70	3.51
1/29	1	29	70	2.80

acid relates to pH by (16):

$$pH = pKa + \log\left(\frac{\alpha}{1-\alpha}\right) \tag{5}$$

one may estimate the pH (pH_{IEP}), at which the gel is in its IEP. Using pKa = 4.25 reported for poly(acrylic acid) gels (17), pH_{IEP} was calculated as 4.25, 3.51 and 2.80, for 10/20-, 4/26-, and 1/29-gels respectively (Table 1).

In Figure 1, the filled symbols show the equilibrium volume V_{eq} of 10/20-gel plotted against pH of the external solution. The swelling results shown in the Figure were repeated three times with excellent reproducibility. The arrow in the Figure points out $pH_{IEP} = 4.25$, at which half of the AAc units is dissociated and the gel is in its IEP. Results of the measurements in distilled water as the swelling medium are also shown in

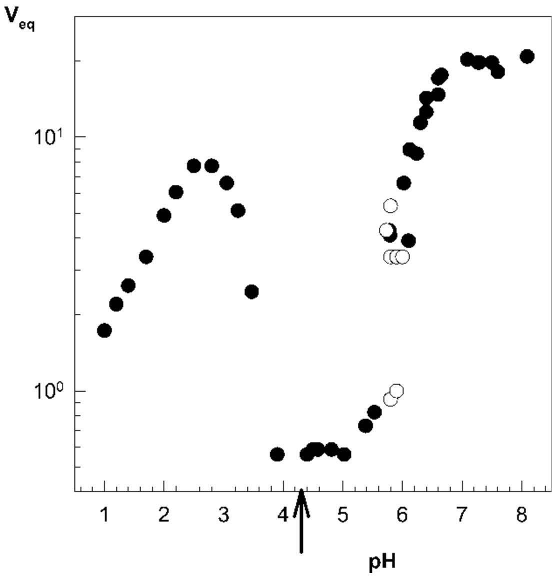

Figure 1. The equilibrium volume V_{eq} of 10/20-gel plotted against pH of the external solution. The arrow indicates $pH_{IEP} = 4.25$. Results of measurements in distilled water are shown by the open symbols.

the Figure by the open symbols. Note that the distilled water was slightly acidic (pH = 5.8–6.0) after a few weeks of swelling time of the gel samples, probably due to the CO_2 absorption from the air. Figure 1 shows that the gel is in a collapsed state in the range of pH between 3.9 and 5.1, while it rapidly swells as the pH is changed outside this region. Thus, 10/20-gel assumes compact conformation not only at pH_{IEP}, but it remains collapsed over a wide range of pH including pH_{IEP}. Figure 1 also shows that the gel undergoes a first-order volume phase transition at $pH = 5.85 \pm 0.05$. Interestingly, we observed that the gel immersed in distilled water changed from a swollen to collapsed state with increasing swelling time due to the simultaneous decrease in pH because of the CO_2 absorption of water. For example, the gel sample in distilled water at pH = 5.9 exhibited a relative volume of 3.4, while after a few days, if pH attained the value 5.8, it occupied a volume of only 0.9. This clearly demonstrates the occurrence of a first-order volume phase transition in the gel at $pH = 5.85 \pm 0.05$. A rapid swelling transition was also observed around pH = 3.7, as seen in the Figure. The pH dependent swelling behavior of 10/20 gel was also measured at 50°C. The results showed that the temperature has no effect on the phase transition in gels at pH = 5.85. This indicates that the hydrogen bonding interactions do not have a dominant effect for the observed phase transition.

The modulus of elasticity of 10/20-gel was measured both at the state of gel preparation and at the equilibrium swollen state in water of various pH, denoted by G_o and G, respectively. Assuming phantom network behavior ($\phi = 4$), $G_o = 2.2$ kPa found by the measurements together with Equation (4) give the effective crosslink density ν_e of the network as $48\ \mathrm{mol \cdot m^{-3}}$. The swollen state moduli G of 10/20-gels are shown in Figure 2 by the filled symbols plotted against pH of the solution. The variation of G with pH is mainly due to the simultaneous change of the gel volume. As seen by the open symbols in the Figure, the effective crosslink density ν_e, calculated using the moduli data together with Equation (3), decreases slightly from 60 to $48\ \mathrm{mol \cdot m^{-3}}$ as

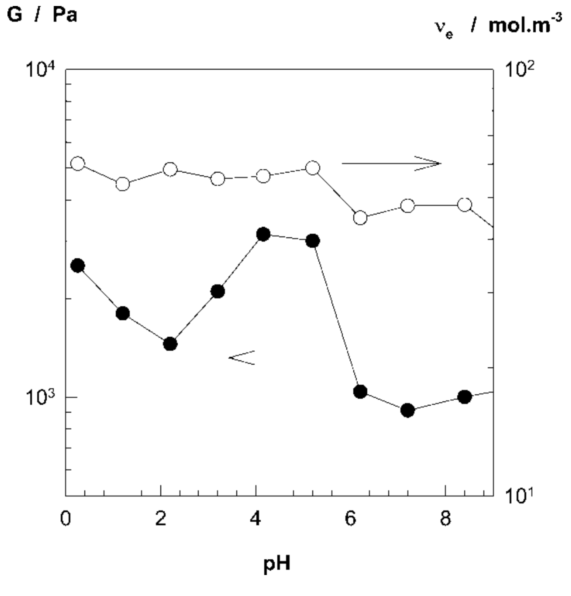

Figure 2. The swollen state modulus G (filled symbols) and the effective crosslink density ν_e (open symbols) of 10/20-gels shown as a function of pH of the solution.

pH is increased from 0 to 8.4. This change in ν_e depending on pH may be attributed to the non-Gaussian elasticity of the network chains in swollen hydrogels (18), and to specific interactions in the gel phase between polymer segments and mobile ions.

Figure 3 shows the equilibrium volume V_{eq} of the hydrogels with three different molar ratios of MAPTAC/AAc units plotted against pH of the external solution. Filled symbols are the results of measurements in water while open symbols are those measured in concentrated (1 M) NaCl solutions. The arrows in the Figures indicate pH_{IEP} values of the hydrogels calculated using Equation (5). Although the hydrogels consist of various proportions of MAPTAC and AAc units, they show similar trends by changing pH of

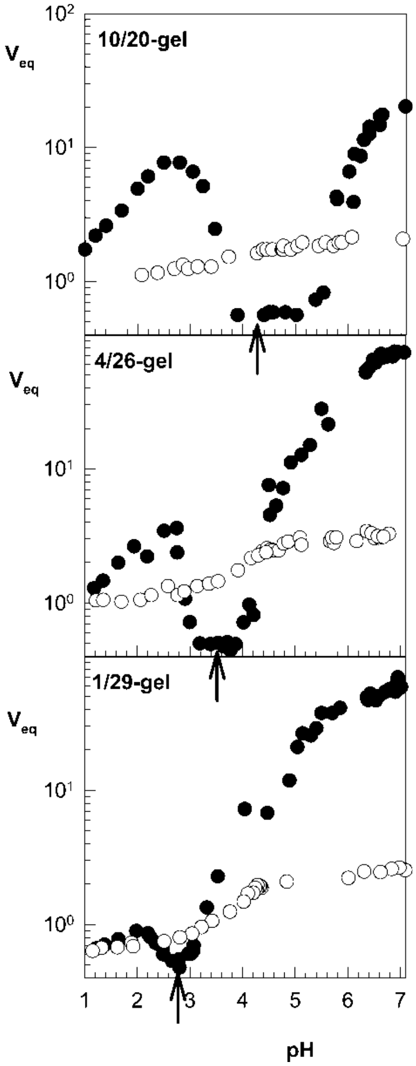

Figure 3. The equilibrium volume V_{eq} of the hydrogels with three different molar ratios of MAPTAC/AAc units shown as a function of pH of the external solution. Filled symbols are the results of measurements in water while open symbols are those measured in concentrated (1 M) NaCl solutions. The arrows in the Figures indicate pH_{cr} values of the hydrogels calculated using Equation (5).

the solution. As the pH increases from 1, V_{eq} first increases and reaches a maximum value at a certain pH. Then, it decreases again with a further increase in pH and attains a minimum value of $V_{eq} \cong 0.5$ around the IEP. The volume of the collapsed gel remains constant over a certain range of pH. After passing this collapsed plateau region, the gel reswells again up to $\mathrm{pH} = 7.1$. The results of measurements above $\mathrm{pH} > 7.1$ were not reproducible, probably due to the hydrolysis of AAm units into AAc units (19, 20). Although the shape of the swelling curves is similar for all the gel samples, distinct differences depending on the gel composition are observable. 1) The collapsed plateau becomes shorter as the MAPTAC content of the hydrogels decreases and, at 1% MAPTAC (1/29-gel), it becomes a point at $\mathrm{pH_{IEP}} = 2.8$. 2) Decreasing MAPTAC content shifts the collapsed region of gels toward a lower pH range. 3) The larger the MAPTAC content, the larger is the gel volume in acidic solutions. 4) The reswelling of the collapsed gel occurs as a first-order phase transition in 10/20- and 4/26-gels at $\mathrm{pH} = 5.85$ and 4.35, respectively, while 1/29-gel reswells continuously beyond the IEP.

In contrast to the non-monotonic swelling behavior of gels in water, the gel volume in 1 M NaCl increases continuously as pH is increased up to about 6, but then it remains constant (Figure 3). Because all the electrostatic interactions are screened at such a high salt concentration, the variation of gel volume with pH can be attributed to structural differences of the gels depending on pH of the solution. Moreover, comparison of the gel volumes recorded in water at the IEP's with those in 1 M NaCl shows that the gel at the IEP is in a much more compact state than in a concentrated salt solution. This indicates that the polyampholyte attraction in the hydrogel is strong enough to cause a complete collapse in the gel at the IEP. In a concentrated NaCl solution, however, although there is no extra repulsion in the gel due to the charge imbalance, the network chains cannot come close enough because they are restricted by polymer connectivity and crosslinks.

The results in Figure 3 also indicate that, at a given pH, the hydrogel outside the collapsed plateau region is less swollen in 1 M NaCl than in water, due to the screening of electrostatic interactions. This is a characteristic of polyelectrolyte hydrogels. The antipolyelectrolyte effect is observable around the plateau region, where the gel occupies a larger volume in 1 M NaCl than in water. This behavior is also illustrated in Figure 4, where V_{eq} is plotted against the concentration of NaCl solution. 10/20-gel at $\mathrm{pH} = 2.7$ as well as 1/29-gel at $\mathrm{pH} = 6.8$ behave as typical polyelectrolytes, while the same gels at $\mathrm{pH} = 4.1$ and 2.8, respectively, exhibit antipolyelectrolyte behavior. Typical polyelectrolyte behavior of hydrogels is due to the decrease in the concentration difference of counterions inside and outside the hydrogel as the salt concentration in the external solution is increased. Moreover, the antipolyelectrolyte behavior appears due to the screening of the opposite charges in the gel by the mobile ions and unfolding of the compact conformation.

In the following paragraphs, the swelling behavior of the hydrogels was analyzed within the framework of the Flory-Rehner theory of swelling equilibrium including the ideal Donnan equilibria. According to the Flory-Rehner theory, the osmotic pressure π of a gel is the sum of three contributions (21, 22):

$$\pi = \pi_{mix} + \pi_{el} + \pi_{ion} \tag{6}$$

where π_{mix}, π_{el}, and π_{ion} are the osmotic pressures due to polymer-solvent mixing (*mix*), due to deformation of network chains to a more elongated state (*el*), and due to the nonuniform distribution of mobile counterions between the gel and the solution (*ion*), respectively. Osmotic pressure π of a gel determines whether the gel tends to expand or to shrink. When nonzero, π provides a driving force for gel volume change. Solvent

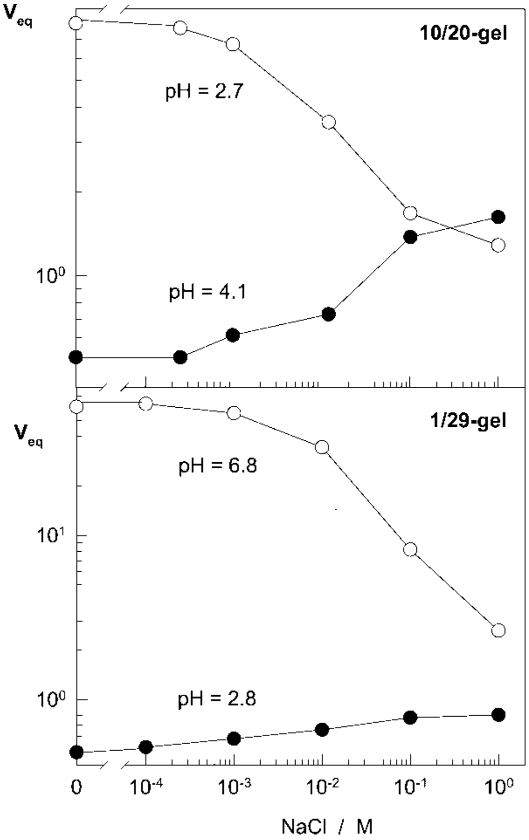

Figure 4. The equilibrium volume V_{eq} of 10/20-gels (upper Figure) and 1/29-gels (lower Figure) plotted against the concentration of NaCl solution. pH of the external solutions are indicated.

moves into or out of the gel until π is zero, i.e., until the forces acting on the gel are balanced. According to the Flory-Huggins theory, π_{mix} is given by (13):

$$\pi_{mix} = -\frac{RT}{\bar{V}_1}\left(\ln(1-\nu_2)+\nu_2+\chi\nu_2^2\right) \tag{7}$$

where χ is the polymer-solvent interaction parameter, $\bar{V}_1$ is the molar volume of solvent (18 mL/g), R and T are in their usual meaning. To describe the elastic contribution π_{el}, we will use here the simplest phantom network model to describe the behavior of our gels (13):

$$\pi_{el} = -0.5\nu_e RT(\nu_2)^{1/3}(\nu_2^0)^{2/3} \tag{8}$$

Ionic contribution π_{ion} to the swelling pressure is caused by the concentration difference of counterions between the gel and the outer solution.

$$\pi_{ion} = RT\sum_i\left(C_i^g - C_i^s\right) \tag{9}$$

where C_i is the mobile ion concentration of species i, the superscripts g and s denote the gel and solution phases, respectively. To evaluate π_{ion}, we consider a polyampholyte gel, consisting of AAm, MAPTAC and AAc units, immersed in an infinite volume of an aqueous solution of HCl and NaCl. Thus, the mobile counterions existing in this system are H^+, Na^+, and Cl^- ions. We define the total concentration of HCl and NaCl in the external solution by C^s_{salt}. The local electroneutrality conditions in both gel and solution phases give the equalities:

$$C^s_{H^+} + C^s_{Na^+} = C^s_{Cl^-} = C^s_{salt} \tag{10a}$$

$$C^g_{H^+} + C^g_{Na^+} + C_B = \alpha C_A + C^g_{Cl^-} \tag{10b}$$

where C_A and C_B are the concentrations of the AAc and MAPTAC units in the gel phase, respectively. Moreover, the ideal Donnan equilibria for univalent salts require the following equalities:

$$C^g_{Na^+} C^g_{Cl^-} = C^s_{Na^+} C^s_{Cl^-} \tag{11a}$$

$$C^g_{H^+} C^g_{Cl^-} = C^s_{H^+} C^s_{Cl^-} \tag{11b}$$

Solution of (Equations 10–11) for the mobile ion concentrations both in the gel and in the solution phases and substituting these concentrations into Equation (9) leads to

$$\pi_{ion} = RT\sqrt{(\alpha C_A - C_B)^2 + (2C^s_{salt})^2} - 2RTC^s_{salt} \tag{12}$$

At the swelling equilibrium, the total osmotic pressure π becomes equal to zero. Thus, using Equations (7), (8), and (12), the equilibrium swelling condition of polyampholyte gels is given by:

$$\ln(1 - \nu_2) + \nu_2 + \chi\nu_2^2 + 0.5\nu_e\bar{V}_1(\nu_2)^{1/3}(\nu_2^0)^{2/3} - \bar{V}_1\sqrt{(\alpha C_A - C_B)^2 + (2C^s_{salt})^2} + 2\bar{V}_1 C^s_{salt} = 0 \tag{13}$$

An important parameter appearing in Equation (13) is the dissociation degree α of AAc units in the gel. Since poly(acrylic acid) is a weak acid, its dissociation is expressed as:

$$K_a = \frac{C_{Ac^-} C^g_{H^+}}{C_A - C_{Ac^-}} \tag{14}$$

where K_a is the dissociation constant and C_{Ac^-} is the concentration of dissociated acid groups (Ac^-). Since $\alpha \equiv C_{Ac^-}/C_A$, i.e.,

$$\alpha = \frac{K_a}{K_a + C^g_{H^+}} \tag{14a}$$

the evaluation of α requires the concentration of H^+ ions in the gel phase $C^g_{H^+}$. Thus, according to Equations (13) and (14a), the swelling behavior of MAPTAC/AAc hydrogels is mainly dictated by pH inside the gel solution. Using the local charge electroneutrality conditions (Equations (10a)) and (10b)), the ideal Donnan equilibria (Equations (11a)) and (11b)) and Equation (14), we obtained a third order polynomial equation for calculation of $C^g_{H^+}$:

$$C^g_{H^+}{}^3 + (K_a + C_B C^s_{H^+}/C^s_{salt}) C^g_{H^+}{}^2 - [K_a(C_A - C_B) C^s_{H^+}/C^s_{salt} + C^s_{H^+}{}^2] C^g_{H^+} - K_a C^s_{H^+}{}^2 = 0 \tag{15}$$

Note that the calculations as described above, but in the presence of NaOH instead of HCl, lead to the same equations except that C^s_{salt} has to be redefined as the total concentration of NaOH + NaCl in the external solution. Equations similar to Equation (15) were reported before for anionic hydrogels with weak acidic functional groups (23), as well as for polyampholyte hydrogels with both weak cationic and anionic units (11). Equation (15) contains the ionic comonomer concentrations C_A and C_B in the gel phase. Defining f_- and f_+ as the mole fractions of AAc and MAPTAC units in the network, they are given by:

$$C_A = f_- \frac{\nu_2}{\bar{V}_r} x 10^3 \tag{16a}$$

$$C_B = f_+ \frac{\nu_2}{\bar{V}_r} x 10^3 \quad \text{(in M)} \tag{16b}$$

where $\bar{V}_r$ is the molar volume of polymer units. As seen from Equations 15–16, the solution of Equation (15) requires the polymer concentration in the gel ν_2, which is determined by Equation (13). Therefore, Equations (13) and (15) were solved simultaneously for both H^+ concentrations in the gel $C^g_{H^+}$ and the polymer concentration ν_2. In the following, we solved Equation (13) numerically with the bisection method by systematic variation of $C^g_{H^+}$, until $C^g_{H^+}$ satisfies the condition given by Equation (15). For calculations, C^s_{salt} was taken as the independent parameter, which was varied in our experiments. The solution of the equations requires the values of the parameters ν_e, $\bar{V}_r$, ν_2^0, and χ, characterizing the network and the extent of the network-solvent interactions. Using the molecular weight of AAm, AAc, and MAPTAC units (71, 72, and 221 g/mol, respectively) together with the polymer density (1.35 g/mL (8)), $\bar{V}_r$ was calculated as $\bar{V}_r = 36.8 + 163.5\, f_+ + 53.3\, f_-$ (mL/mol). From the modulus of elasticity of 10/20-gel, ν_e was calculated as 48 mol/m^3, which was used for all calculations. The volume fraction of crosslinked polymer after preparation, ν_2^0, was calculated from the initial monomer concentration (5 w/v%) together with the polymer density, as 0.037. The χ parameter value for PAAm-water system was evaluated before from the swelling and elasticity data for uncharged PAAm hydrogels swollen in water (7, 24). A best-fit value for χ of 0.48 was obtained. This value of χ parameter provided a good fit to the experimental swelling data of acrylamide-based anionic, cationic, and polyampholyte hydrogels of various compositions (7). For the following calculations, χ was held constant at this value. It must be pointed out that the χ parameter is independent on the number of the charges created on the network chains, since this effect is included in Equation (12). Respective calculations using the parameters given above yield, under certain conditions, three sets of solutions for Equations (13) and (15), indicating an instability in the gel. In these cases, the excess chemical potential of the polymer segments, $\Delta\mu_2$, was calculated (25). The solution that gives a smaller value of $\Delta\mu_2$ was taken as the stable gel phase. If two solutions give the same value of $\Delta\mu_2$, then a phase transition is predicted.

Simulation results of Equations (13) and (15) for 10/20-, 4/26-, and 1/29-gels immersed in water of various pH are shown in Figure 5. Here, the gel volume V_{eq} ($=\nu_2^0/\nu_2$) and the pH in the gel phase pH$_{\text{in}}$ ($=10^{-C^g_{H^+}}$) are plotted against pH of the external solution. Comparison of the theoretical V_{eq} vs. pH curves in Figure 5 with the experimental data for the same set of gels given in Figure 3 clearly shows that the theory qualitatively predicts the experimental behavior of gels. The collapsed plateau observed in 10/20- and 4/26-gels, as well as the first-order phase transitions observed for these gels were also predicted by the theory. In agreement with the experiments, the

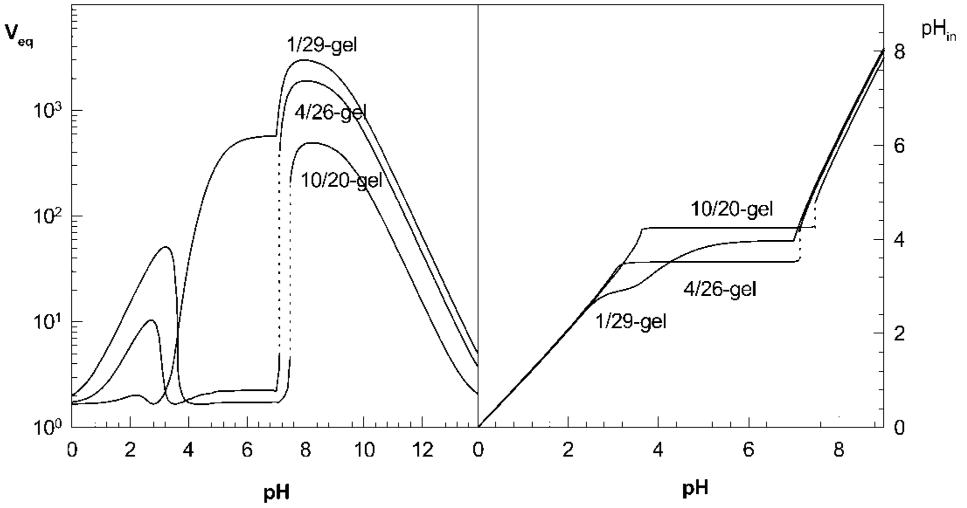

Figure 5. The equilibrium volume V_{eq} of the hydrogels with three different molar ratios of MAPTAC/AAc units and pH in the gel solution (pH_{in}) shown as a function of pH of the external solution. Phase transition regions are indicated by the vertical dotted lines. Calculations were using Equations (13) and (15).

plateau shifts toward a lower range of pH as the MAPTAC is decreased and it disappears for the gel with 1% MAPTAC content.

To explain the physical meaning of the predictions, we will first consider the 10/20-gel immersed in water. At a low pH, the gel network exists as a cationic polyelectrolyte because of suppression of its AAc groups. At pH = 0, the dissociation degree α of AAc is almost zero, that is, the cationic gel exhibits a maximum charge density ($f_+ = 0.10$). However, it remains collapsed due to the high H^+ concentration in the solution $C^g_{H^+}$, which totally screens the MAPTAC groups. As pH increases from 0 to 3.2, the gel swells due to the decrease of $C^g_{H^+}$ from 10° to 6×10^{-4} M. Although the simultaneous increase of α in this range of pH decreases the net charge of the gel, ($C_B - \alpha\ C_A$), this effect is negligible and, decreasing H^+ concentration dominates the swelling process. However, above pH = 3.2, since H^+ concentration is low, decreasing gel charge density with rising pH dominates the swelling process so that the gel deswells continuously until the IEP, i.e., until $pH_{IEP} = 4.25$, at which the network is electroneutral and adopts a compact conformation.

It should be noted that, in the range of pH between 3.2 and 4.25, the acrylate (Ac^-) concentration is much larger than the H^+ concentration in the gel solution. Therefore, the local electroneutrality in the gel phase is provided by the MAPTAC units acting as the counterions of Ac^- units. As pH approaches to pH_{IEP}, more and more MAPTAC units are occupied by Ac^- units formed by the dissociation of AAc groups. At the IEP, both the concentrations of the dissociated AAc and MAPTAC units in the gel become 3.5×10^{-2} M compared to $C^g_{H^+} = 5.6 \times 10^{-5}$ M. Thus, H^+ concentration in the gel at the IEP is about thousand-fold smaller than the concentration of fixed Ac^- groups. Since no more MAPTAC units are available for the AAc units to dissociate beyond the IEP, the dissociation of AAc stops so that both the gel volume and pH in the gel remain unchanged until pH = 7.48. Thus, along the collapsed region of gel, pH_{in} remains constant at pH_{IEP}. At pH = 7.48, the osmotic pressure due to the concentration difference of H^+ and Na^+ ions between the gel and outer solution exceeds the negative osmotic pressure due to the gel rubber-like elasticity holding the gel in a collapsed state. As a result, the gel undergoes a first-order swelling transition, during which the gel network transforms from electroneutral to anionic one. Increase of the gel volume during swelling decreases the H^+ concentration in the gel, which enhances the ionization of AAc groups and results further expansion of the anionic network. The dissociation degree α approaches to unity at $pH = 8.2$ so that between $pH = 8.2$ and 10, the anionic gel volume remains almost constant. Above $pH = 10$, the gel deswells again due to the increasing concentration of ions in the solution which screens the Ac- groups responsible for gel swelling.

As the MAPTAC content is decreased from 10 to 1%, the charge density of the cationic gel at a low pH also decreases so that the gel volume in acidic solutions decreases. Simultaneously, decreasing MAPTAC content moves the IEP toward a lower pH so that the gel remains collapsed in a lower range of pH. For the 1/29 gel, IEP occurs at $pH = 2.80$. Since there are enough H^+ ions in the gel at this value of pH, the dissociation of AAc continuous beyond the IEP and no plateau appears in the swelling curve.

Comparison of the experimental data with the theory also indicates that the theory predicts much larger gel volumes than observed by the experiments. Also, the range of pH in which the gels are in a collapsed state, as well as the volume of the collapsed gels predicted by the theory are also much larger than found by the experiments. These discrepancies may originate from various nonidealities. The swelling model assumes that all the fixed charges inside the gel and therefore, their counterions are effective in the gel swelling. Recent experimental and theoretical results indicate however the existence of "osmotically passive" counterions inside the swollen gel which do not contribute to the swelling process (2, 8, 24, 26, 27). We have shown that a large fraction of counterions in ionic gels is ineffective in the swelling process (24). Since the model neglects this nonideality, it predicts larger gel volumes than observed by the experiments. Moreover, gel heterogeneities may also be responsible for these deviations. As reported before (28, 29), the gel formation process by free-radical mechanism necessarily leads to inhomogeneous gels with a nonuniform distribution of crosslinks. Thus, it consists of highly crosslinked domains separated by the dilute regions. The counterions in the highly crosslinked (less swollen) regions of the gel may condense on the network chains and become passive in the gel swelling. Inhomogeneous distribution of the ionic comonomer units along the network chains may also contribute to the observed discrepancies. The attraction between charge density fluctuations due to the gel inhomogeneities may lead to a chain collapse and form a much dense globule than predicted by the theory. Furthermore, the use of a single dissociation constant K_a for acrylic acid units is also questionable. K_a may vary depending on pH and salt concentration and, it is also sensitive to the local environment of AAc groups, as each ionized AAc group is known to decrease the tendency of its neighbors to ionize (16). Finally, the swelling calculations based on the ideal Donnan theory are not capable of describing antipolyelectrolyte behavior of the hydrogels in salt solutions. This is also illustrated in Figure 6, where the experimental swelling curves (solid lines) of 10/20-gel at $pH = 2.7$ and 4.1 are compared with the calculation results (dotted curves). In this Figure, the gel volume calculated by the theory ($V_{eq,theory}$) was adjusted to fit the experimental V_{eq} data obtained at $pH = 2.7$. Although the theory qualitatively reproduces the deswelling curves of gels in NaCl solutions, the swelling of balanced hydrogels cannot be predicted. By inserting the Debye-Hückel theory of electrolyte solutions into the swelling model

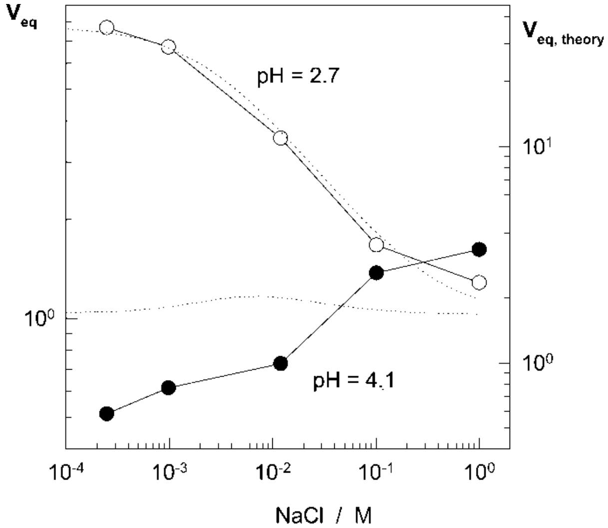

Figure 6. The experimental swelling curves (solid lines) of 10/20-gels at pH = 2.7 and 4.1 in NaCl solutions of varying concentration are shown in comparison with the predictions of the theory (dotted curves). The gel volume calculated using the theory ($V_{eq,theory}$) was adjusted to fit the experimental V_{eq} data obtained at pH = 2.7.

(6), we were able to account for the antipolyelectrolyte behavior of the hydrogels. However, such calculations provided poor agreement with the experimental data at the expense of greater numerical complexity and larger number of parameters. The simple swelling model presented here well describes the equilibrium swelling behavior of polyampholyte hydrogels under various experimental conditions.

Conclusions

The swelling behavior of AAm-based polyampholyte hydrogels was investigated. Three sets of hydrogels containing 70 mol% AAm and 30 mol% MAPTAC + AAc of varying mole ratios were prepared. The variations of the hydrogel volume in response to changes in pH, and salt concentration were measured. As pH increases from 1, the hydrogel volume V_{eq} in water first increases and reaches a maximum value at a certain pH. Then, it decreases again with further increase in pH and attains a minimum value around the IEP. After passing the collapsed plateau region, the gel reswells again up to pH = 7.1. The reswelling of the collapsed gels containing 10 and 4% MAPTAC occurs as a first-order phase transition at pH = 5.85 and 4.35, respectively, while the hydrogel with 1% MAPTAC reswells continuously beyond the IEP. A qualitative agreement was found between the experimental behavior of the hydrogels and the predictions of the Flory-Rehner theory including the ideal Donnan equilibria.

Acknowledgments

Work was supported by the Scientific and Technical Research Council of Turkey (TUBITAK), TBAG –105T246.

References

1. Baker, J.P., Stephens, D.R., Blanch, H.W., and Prausnitz, J.M. (1992) *Macromolecules*, 25: 1955.
2. Baker, J.P., Blanch, H.W., and Prausnitz, J.M. (1995) *Polymer*, 36: 1061.
3. Nisato, G., Munch, J.P., and Candau, S.J. (1999) *Langmuir*, 15: 4236.
4. Zhai, M., Chen, Y.C., Yi, M., and Ha, H. (2004) *Polym. Int.*, 53: 33.
5. Takeoka, Y., Berker, A.N., Du, R., Enoki, T., Grosberg, A., Kardar, M., Oya, T., Tanaka, K., Wang, G., Yu, X., and Tanaka, T. (1999) *Phys. Rev. Lett.*, 82: 4863.
6. English, A.E., Tanaka, T., and Edelman, E.R. (1998) *Macromolecules*, 31: 1989.
7. Baker, J.P., Hong, L.H., Blanch, H.W., and Prausnitz, J.M. (1994) *Macromolecules*, 27: 1449.
8. Durmaz, S. and Okay, O. (2000) *Polymer*, 41: 3693.
9. Annaka, M. and Tanaka, T. (1992) *Nature*, 355: 430.
10. Annaka, M. and Tanaka, T. (1994) *Phase Transit.*, 47: 143.
11. Mafe, S., Manzanares, J.A., English, A.E., and Tanaka, T. (1997) *Phys. Rev. Lett.*, 79: 3086.
12. Sayil, C. and Okay, O. (2001) *Polymer*, 42: 7639.
13. Flory, P.J. (1953) *Principles of Polymer Chemistry*; Cornell University Press: Ithaca, NY.
14. Treloar, L.R.G. (1975) *The Physics of Rubber Elasticity*; University Press: Oxford.
15. Mark, J.E. and Erman, B. (1988) *Rubberlike Elasticity. A Molecular Primer*; Wiley-Interscience: NY.
16. Miller, M.L. (1964) Acrylic acid polymers. In *Encyclopedia of Polymer Science and Technology*; Mark, H.F., Gaylord, N.G., and Bikales, N.M. (eds.), Interscience: NY; Vol. 1, 197–226.
17. Ende, M.T.A. and Peppas, N.A. (1996) *J. Appl. Polym. Sci.*, 59: 673.
18. Gundogan, N., Melekaslan, D., and Okay, O. (2002) *Macromolecules*, 35: 5616.
19. Ilavsky, M., Hrouz, J., Stejskal, J., and Bouchal, K. (1984) *Macromolecules*, 17: 2868.
20. Kizilay, M.Y. and Okay, O. (2003) *Polymer*, 44: 5239.
21. Flory, P.J. and Rehner, J., Jr. (1943) *J. Chem. Phys*, 11: 521.
22. Frenkel, J. (1940) *Rubber Chem. Technol.*, 13: 264.
23. English, A.E., Tanaka, T., and Edelman, E.R. (1996) *J. Chem. Phys*, 105: 10606.
24. Okay, O. and Durmaz, S. (2002) *Polymer*, 43: 1215.
25. Okay, O. and Gundagan, N. (2002) *Macromol. Theory Simul.*, 11: 287.
26. Skouri, R., Schosseler, F., Munch, J.P., and Candau, S.J. (1995) *Macromolecules*, 28: 197.
27. Okay, O., Sarisik, S.B., and Zor, S.D. (1998) *J. Appl. Polym. Sci.*, 70: 567.
28. Shibayama, M. (1998) *Macromol. Chem. Phys*, 199: 1.
29. Kizilay, M.Y. and Okay, O. (2003) *Macromolecules*, 36: 6856.